Calcium Specificity of the Antigen-Induced Channels in Rat Basophilic Leukemia Cells†

Ayus Corcia,‡ Israel Pecht,*,§ Stefan Hemmerich,§ Sophia Ran,‡ and Benjamin Rivnay‡
Departments of Membrane Research and Chemical Immunology, The Weizmann Institute of Science, Rehovot 76100, Israel
Received December 21, 1987; Revised Manuscript Received April 14, 1988

ABSTRACT: Ion channels, activated upon IgE–Fc_ϵ receptor aggregation by specific antigen, were studied in micropipet-supported lipid bilayers. These bilayers were reconstituted with purified IgE–Fc_ϵ receptor complex and the intact 110-kDa channel-forming protein, both isolated from plasma membranes of rat basophilic leukemia cells (line RBL-2H3). In order to identify the current carrier through these ion channels and to determine their ion selectivity, we investigated the currents flowing through the IgE–Fc_ϵ receptor gated channels in the presence of a gradient of Ca^{2+} ions. Thus, the solution in which the micropipet-supported bilayer was immersed contained 1.8 mM $CaCl_2$, while the interior of the micropipet contained 0.1 μM Ca^{2+} (buffered with EGTA). Both solutions also contained 150 mM of a monovalent cation chloride salt (either K^+ or Na^+). The currents induced upon specific aggregation of the IgE (by either antigen or anti-IgE antibodies) were examined over a range of potentials imposed on the bilayer. The type of conductance event most frequently observed under the employed experimental conditions was a channel that has a slope conductance of 3 pS and a reversal potential practically identical with the calculated value for the reversal potential of calcium (134 ± 11 mV in the presence of sodium, 125 ± 13 mV in the presence of potassium). These results indicate that this channel is highly selective for calcium against the monovalent cations sodium and potassium. This same channel has a conductance of 4–5 pS in the presence of symmetrical solutions containing only 100 mM $CaCl_2$ and 8 pS in the presence of 0.5 M NaCl with no calcium. A second type of conductance event appears under all the above-described conditions at much lower frequency (<10% of all the resolved events). These events have a higher conductance (10–20 pS in the presence of different concentrations of calcium ions, 25 pS in the presence of 0.5 M sodium chloride with no calcium) but are less selective for calcium against either sodium or potassium, as determined from their reversal potential. Comparison of the conductance changes observed in the above experiments with the reported values for the amounts of Ca^{2+} ions taken up by the intact RBL-2H3 cells upon antigen stimulation suggests that these antigen-induced calcium channels can account for the increase in intracellular calcium that occurs upon antigen stimulation of these cells.

The calcium dependence of IgE-mediated degranulation of mast cells and basophils is amply documented (Mongar & Schild, 1958; Lichtenstein & Osler, 1964; Foreman & Mongar, 1972; Foreman, 1981). This notion has, however, been challenged to some extent in recent years since for some types of mast cells (e.g., from rat peritoneum) experimental protocols were designed where mediator release could be attained in the apparent absence of extracellular calcium ions (Enis et al., 1980; Fernandez et al., 1984). A rationale for these observations may be found in the operation of different, possibly parallel, pathways that link a given stimulus applied at the cells' membrane to the eventual mediator secretion (Gomperts & Fewtrell, 1986). The existence of different coupling processes for distinct stimuli has already been indicated, for example, in the case of IgE-mediated versus polyamine-induced secretion (Foreman & Mongar, 1972; Douglas & Ueda, 1973; Cochrane et al., 1982; Saito et al., 1987). Whereas the first was shown to depend on extracellular calcium, the latter was not. These observations were indeed assigned to the involvement of two distinct mechanistic routes (Foreman, 1981; Saito et al., 1987). Evidence is also emerging for the possibility that, in a given type of mast cell, one particular stimulus may also be transmitted by alternative pathways when appropriately modulated. For example, phorbol esters, which are effective activators of protein kinase C, were shown to enable IgE-mediated degranulation without a detectable increase in cytosolic free calcium (Sagi-Eisenberg et al., 1985; Reck et al., 1986). Such potential flexibility in coupling processes, superimposed on the known heterogeneity of mast cells derived from different organs or more so from diverse species (Befus et al., 1986), would evidently complicate and hamper a mechanistic analysis.

The use of a well-defined cell line has been found to be helpful in circumventing, at least partly, the above-mentioned difficulties. The leukemic line of rat mast cells (RBL-2H3)[1] was found to respond well to IgE-mediated stimuli but hardly at all to polyamines (Eccleston et al., 1973; Fewtrell et al., 1979; Crews et al., 1981; Seldin et al., 1985). A significant amount of our current biochemical understanding of the IgE-mediated stimulus and, in particular, the identification and isolation of components involved in it, were made feasible by using these cells (Metzger et al., 1986). The IgE-mediated secretion from RBL-2H3 cells was shown to strictly require extracellular Ca^{2+} ions. Measurements, both by the $^{45}Ca^{2+}$ tracer and by fluorescent calcium indicators, have suggested

† This research was supported by NIH Grant ALY1RO1 AI 22669 (I.P. and B.R.), by the Fund for Basic Research administered by the Israel National Academy of Sciences and Humanities (A.C.), by the Victor and Marie Adda Fund (B.R.), and by grants of the Minerva Foundation (A.C. and B.R.).
‡ Department of Membrane Research.
§ Department of Chemical Immunology.

[1] Abbreviations: CHAPS, 3-[(3-cholamidopropyl)dimethylammonio]-1-propanesulfonate; DNP, 2,4-dinitrophenyl; $Fc_\epsilon R$, high-affinity receptor for IgE; IgE–$Fc_\epsilon R$, complex of the receptor for IgE with its ligand IgE; RBL-2H3, rat basophilic leukemia, subline 2H3.

0006-2960/88/0427-7499$01.50/0

that the transient rise in cytosolic free calcium that occurs as part of the coupling process between antigen stimulus and mediator secretion (Crews et al., 1981; Beaven et al., 1984; Sagi-Eisenberg et al., 1985; Mohr & Fewtrell, 1987; Ran & Rivnay, 1988) involves a net uptake of this cation. The role of alternative second messengers, which may induce calcium release from intracellular stores or which may not require a rise in cytosolic calcium altogether, has not yet been resolved for the RBL-2H3 cells.

Earlier studies have provided evidence for the presence of antigen-activated ion channels in the plasma membrane of these cells (Mazurek et al., 1984). The component forming this channel has been suggested to be the 110-kDa protein now isolated from plasma membranes of the RBL-2H3 cells (Hemmerich & Pecht, 1988). Studies performed on lipid bilayers coreconstituted with the purified Fc_ϵ receptor ($Fc_\epsilon R$) and preparations enriched in the channel-forming protein suggested that these two components are the minimal requirement for forming an open ion channel upon receptor aggregation (Corcia et al., 1986). No channel activity could be induced in membranes containing the IgE–$Fc_\epsilon R$ complex only, indicating that this component itself has no channel-forming properties. Rather, it probably functions as a transducer for the former.

In this study we have concentrated on resolving the ion specificity of this $Fc_\epsilon R$-operated channel, using the highly purified channel-forming protein isolated as described in the preceding paper. The results indicate that under conditions resembling the physiological Ca^{2+} ion gradient across the bilayer the channel is specific for calcium ions.

Experimental Procedures

Materials. 3-[(3-Cholamidopropyl)dimethylammonio]-1-propanesulfonate (CHAPS), cholesterol, egg phosphatidylcholine, and soybean lecithin (Asolectin, type IV-S) were all purchased from Sigma Chemical Co. (St. Louis, MO). Asolectin was further processed as described by Kagawa and Racker (1971). Salts and solvents were all of analytical grade.

Buffers. Four different experimental solutions were used to bathe the bilayers. In experiments performed under symmetrical conditions, the solutions in both the well and the pipet contained either 100 mM $CaCl_2$ or 0.5 M NaCl and 10 mM Tris-HCl, pH 7.4. In experiments where a gradient of calcium concentrations was applied, both solutions contained 150 mM of a monovalent cation chloride salt (either NaCl or KCl) and 5 mM Hepes, pH 7.0 (unless indicated otherwise). In addition, the solution in the well contained 1.8 mM $CaCl_2$ and that in the pipet contained 0.1 μM free Ca^{2+} buffered with EGTA (2 mM $CaCl_2$, 10 mM EGTA). These amounts of $CaCl_2$ and EGTA were calculated by using the values of the dissociation constants given by Fabiato and Fabiato (1975). All the solutions were filtered before use.

Proteins. Mouse monclonal, IgE class 2,4-dinitrophenyl-specific antibodies, secreted by hybridoma cells [HI-DNP-ϵ-26.82; Liu et al. (1980)], were isolated as detailed elsewhere (Holowka & Metzger, 1982). The IgE–$Fc_\epsilon R$ has been purified from RBL-2H3 cells by two steps of affinity chromatography. Throughout this procedure the buffer contained 2 mM phospholipids derived from RBL-2H3 cells and 10 mM CHAPS. The homogeneity of the isolated receptor was similar to that reported earlier (Rivnay et al., 1984). The channel-forming protein has been isolated and purified as described in the preceding paper. $DNP_{16}BSA$ was used for antigenic stimulations.

Reconstitution of Planar Bilayers and Conductance Measurements. The procedure for lipid bilayer formation at the tip of glass micropipets is a variation of that presented by Coronado and Latorre (1983) and has been described earlier (Corcia et al., 1986). Liposomes were prepared from a mixture of lipids (soybean lecithin, egg phosphatidylcholine, and cholesterol, 8:11:1 by weight). This was dried under a stream of nitrogen and then resuspended in a solution containing, in addition to the appropriate salts, ~15 nM of the purified IgE–$Fc_\epsilon R$ complex and ~15 nM of the purified channel-forming protein. These solutions were dialyzed for at least 4 h before being used to resuspend the lipid film. The suspension containing proteins and lipids was sonicated for 1 min. After sonication, 75 μL of the suspension was added to a plastic well of a microtiter plate containing the same volume of the experimental solution, and at least 5 min was allowed for the liposomes to form a monolayer at the air–water interface. At this stage, a glass micropipet with a tip diameter of ~1 μm, placed in the well before adding the liposome suspension, was raised above the interface and slowly reintroduced by a three-dimensional hydraulic micromanipulator. Formation of a bilayer at the micropipet tip was monitored by measuring the changes in its resistance with an EPC-5 patch clamp system (List Electronics, FRG). Once a bilayer was formed, it was clamped at different transmembrane potentials with the patch clamp system. Special care was taken to ensure that the experiments were carried out only at potentials that did not induce instabilities in the bilayer that could be mistaken as channel activity (Corcia & Babila, 1985; Corcia et al., 1986). After recording for a few minutes at such potentials, an IgE cross-linking agent ($DNP_{16}BSA$ or rabbit anti-murine IgE, 5 or 7 nM final concentration, respectively) was added to the well and the recording continued for 10–15 min. The current necessary to clamp the membrane was recorded on an FM tape recorder and analyzed off-line with an IBM PC/AT microcomputer. The recorded currents were low-pass filtered before being digitized by the computer using a 8-pole Bessel filter (Frequency Devices Inc.). The corner frequency was either 300 or 500 Hz, depending on the signal-to-noise ratio of each record. Channel events were then detected and measured by a locally developed software program. Using this program, the operator determines both the amplitude and the open time of each of the events. Sign notations were always such that pipet interior was negative with respect to the grounded well. Channel opening appears as a downward deflection in the current traces, corresponding to current influx into the pipet. Experiments were ordinarily terminated by the addition of lanthanum (10 μM) or cromolyn (100 μM) to the bath compartment. This, with no exception, resulted in the disappearance of detectable channel activity.

Results

Micropipet-supported bilayers were employed in all the experiments reported below. The membranes were formed from liposomes containing the purified Fc_ϵ receptor–IgE complex and the channel-forming protein. Antigen ($DNP_{16}BSA$, 5 nM) or anti-murine IgE antibodies (7 nM) were used to induce IgE-mediated receptor aggregation and channel activity. Figure 1 shows representative traces of antigen-induced channel activity from two different experiments in which the bilayers separated identical $CaCl_2$ solutions (100 mM), at two different transmembrane potentials. At the protein to lipid ratio employed in these experiments (1.3 mM lipids and 7.5 nM of each protein), channel events appeared sparsely and were separated by long intervals without activity. The concentrations of the proteins were adjusted so that no more than one or two functional channels are present in the reconstituted bilayers. In general, 50–100 single-channel

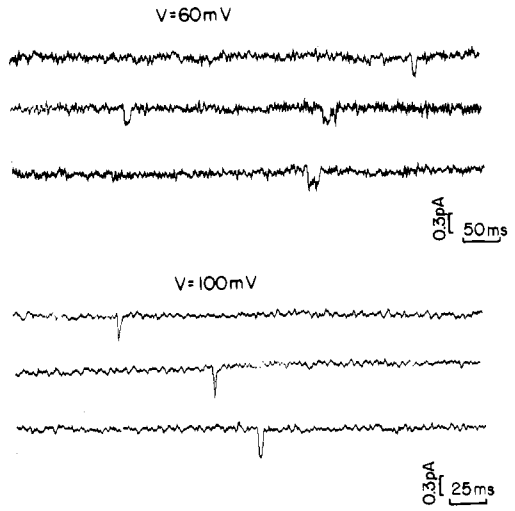

FIGURE 1: Illustrative current traces taken from two different experiments with micropipet-supported lipid bilayers containing both the Fc_ϵ receptor–IgE complex and the channel-forming protein. The IgE is DNP-specific, and conductance was triggered by antigen ($DNP_{16}BSA$). Solutions on both sides of the bilayer contained symmetrical Tris-HCl buffered 100 mM $CaCl_2$.

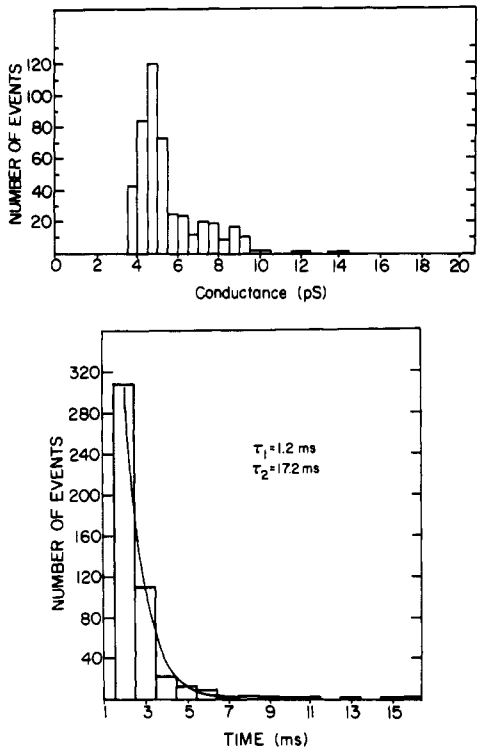

FIGURE 2: Conductance and open-time histograms constructed from antigen-induced single-channel events in micropipet-supported bilayers in the presence of 100 mM $CaCl_2$. Data from six different experiments were pooled together, analyzed, and used to construct these histograms.

events were observed during the 10–15 min of measurements following antigen addition to the well. No conductance changes could be observed during 5–10 min prior to the addition of antigen. The conductance and open-time histograms constructed from events detected in six different experiments performed under such conditions are shown in Figure 2. The histograms derived from each individual experiment show similar distributions. The major peak of conductance was at 4.5–5 pS (Figure 2, top panel). This main population of events accounts for over 90% of all the channels observed. The remaining <10% of the events have a conductance in the range of 10–15 pS. This small population of events with higher

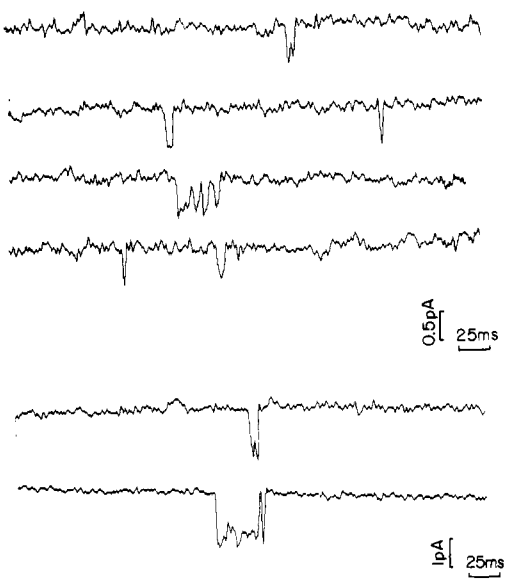

FIGURE 3: Sample traces of antigen-induced channels of the two different amplitudes observed in bilayers containing the $Fc_\epsilon R$–IgE complex and the channel-forming protein in the presence of a calcium concentration gradient. The gradient was made as described under Experimental Procedures in otherwise symmetrical buffer composition (100 mM NaCl, 10 mM Tris-HCl, pH 7.5) maintained in both compartments. Clamp potential was 60 mV, pipet interior negative. Data were filtered at 300 Hz and digitized at 5 kHz. Note the difference in the vertical scale between the four upper records and the lower two.

conductance appeared consistently in all the experiments carried out in the presence of symmetrical solutions containing only calcium (100 mM) and buffer. The open-time histogram of all the events detected in these experiments is shown in the lower panel of Figure 2. Most of the events have open times in the range of 1.5–5 ms. The relatively extensive filtering necessary in order to detect these small currents removes or distorts faster fluctuations of the channels (Nelson, 1986). Consequently, events with open times shorter than 1.5 ms, although observed in these experiments, were not included in the histograms. Events with open times longer than 5 ms (up to 100 ms) were also detected, yet much less frequently. The distribution of open times has been fitted to the sum of two exponential functions having average open times of 1.2 and 17.2 ms, respectively. These results agree well with those obtained before with a much smaller number of channel events (Corcia et al., 1986). Because of the problems inherent in the detection of very short events, the value of the average open time for the fast channel openings must be considered as an upper limit for the real value. Our figures must be seen at this stage as indicating that two exponentials, with average times differing by 1 order of magnitude, are necessary, for the fitting of the experimental distribution of open times.

In order to resolve the ion selectivity of these channels, which cannot be inferred from the results presented above (see Discussion), and to characterize the channel activity under conditions closer to the physiological situation, the following experiments were carried out: Planar bilayers were immersed in symmetrical NaCl solutions (150 mM), in the presence of a concentration gradient of calcium (1.8 mM $CaCl_2$ in the bath versus EGTA-buffered 0.1 μM $CaCl_2$ in the pipet). Since two of the three ions present (sodium and chloride) are at essentially identical concentrations on both sides of the bilayer, the reversal potential derived from the current–voltage relationship of the channel events contains information about the ionic selectivity of the channel, under the conditions employed. Figure 3 presents traces of antigen-activated channel events

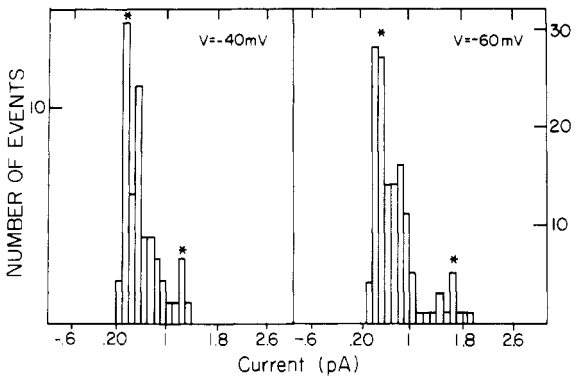

FIGURE 4: Current histograms constructed from antigen-induced single-channel events observed in the same membrane as in the experiments shown in Figure 3 at two different transmembrane potentials. The asterisks (*) indicate the two main peaks used to derive the current–voltage relationships.

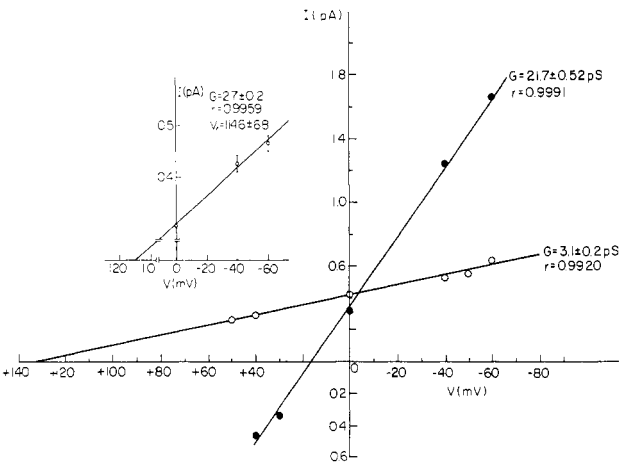

FIGURE 5: Current–voltage plots derived from antigen-induced single-channel events measured in the presence of a calcium concentration gradient (1.8 mM $CaCl_2$ in the well versus 0.1 μM in the pipet). Experimental details are the same as in Figure 3. Data from seven separate experiments were pooled together in order to construct the main plot. Empty points (○) represent the major population of conductance events. Solid points (●) are of the minor population. The extended lines represent the best linear regression fit to the experimental points. For each of the two lines, the slope (channel conductance) and the regression coefficient r are indicated. Inset: Results of similar experiment performed, however, with the purified intact channel-forming protein electroeluted from the 110-kDa band in SDS–PAGE gels. A total of 130 events were analyzed and used in constructing this current–voltage plot.

observed in one experiment of this kind, at a transmembrane potential of 60 mV (pipet interior negative). In every experiment of this series, measurements were performed with at least five different transmembrane potentials (in the range of +50 to −100 mV, pipet interior with reference to the grounded bath). Each potential was maintained for periods ranging from 3 to 10 min. The single-channel events that were detected at each potential appeared with similar frequencies as in the experiments described above. Interestingly, as in the earlier experiments done in symmetric solutions, there were two well-resolved and distinct current levels that occurred randomly throughout the experiments. Events with open times longer than 10 ms were also observed in this series of experiments.

Histograms of channel current amplitudes (not conductances) at two different applied potentials are presented in Figure 4 for the same experiment as that illustrated in Figure 3. Two main populations (marked with * in the figure) are observed in each histogram, one accounting for ~90% of the events. The current values of these two peaks were used to draw the current–voltage plot shown in Figure 5. This figure contains cumulative data obtained in seven separate experiments, all done under the same experimental conditions. In each individual experiment, results were obtained at five or six different voltage values. Each data point presented in the figure is the average of at least four and up to seven values obtained from histograms, similar to those presented in Figure 4, constructed for each separate experiment. The two different populations of events are also evident from the straight lines fitting the points. One of these, with a slope conductance of of 3.1 ± 0.2 pS and a reversal potential of 134.5 ± 11.5 mV (SD), accounts for the main population of events observed in these experiments and corresponds to a calcium-specific channel (see Discussion). The second population of events, representing the less frequent ones, has a slope conductance of 21.7 ± 0.5 pS and a reversal potential of 16.2 ± 1.3 mV, suggesting that a minor population of channels allows the passage of both calcium and monovalent cations, although it shows a marked preference for the former (see Discussion).

In order to establish that the calcium channel activity observed with the isolated 110 kDa polypeptide [cf. Hemmerich & Pecht (1988)] is indeed solely due to this component and not to other potential contaminants, channel activity measurements were carried out with the respective protein band, following additional purification. For this purpose, a 100-fold larger sample than that required for a reconstitution experiment was prepared from the Triton X-100 solubilized fraction of surface-radioiodinated cells by affinity chromatography on cromolyn-BSA-Sepharose and further purification of the protein by nonreducing SDS–PAGE and electroelution of the relevant band, as described in detail in the preceding paper (Hemmerich & Pecht, 1988). Then the electroeluate was supplemented with 0.1 mM total phospholipid, dialyzed extensively, and reconstituted with the $Fc_\epsilon R$–IgE as described under Experimental Procedures. The series of experiments identical with those described above (Figures 3–5) with 150 mM Na^+ and the Ca^{2+} gradient employed these reconstituted vesicles to form the micropipet-supported bilayers. These experiments yielded results very similar to those obtained earlier. As seen in the inset of Figure 5, where a current–voltage plot of these results is presented, a reversal potential of 115 mV was obtained. This is in good agreement with the values obtained with the purified but not electrophoresed preparations (134.5 mV in NaCl, 125.5 mV in KCl). The 50-kDa subunit obtained by elution of the matrices with disulfide-reducing agents (e.g., DTT) was inactive in these experiments. So were also controls eluted from gel slices of either above or below the appropriate band.

A parallel series of experiments was performed under conditions identical with the above, except that potassium instead of sodium was used as the monovalent cation symmetrically present on both sides of the reconstituted bilayer. Antigen-induced channels were observed in six different experiments in the presence of symmetrical 150 mM KCl solutions and the same gradient of $CaCl_2$ as before (1.8 mM in the bath, 0.1 μM in the pipet). Two distinct populations were resolved in the current histograms and were used to obtain the current–voltage relationships of these events (not shown). The calculated slope conductances were 2.7 ± 0.3 and 15.6 ± 0.6 pS (r = 0.994 and 0.997, respectively) and the reversal potentials 125.5 ± 12.9 and 14.2 ± 3.0 mV, respectively. As in the presence of sodium ions and a Ca^{2+} gradient, the small conductance events represent a channel specific for calcium while the second kind of channel, with a higher conductance, allows the passage of both calcium and the monovalent ion present.

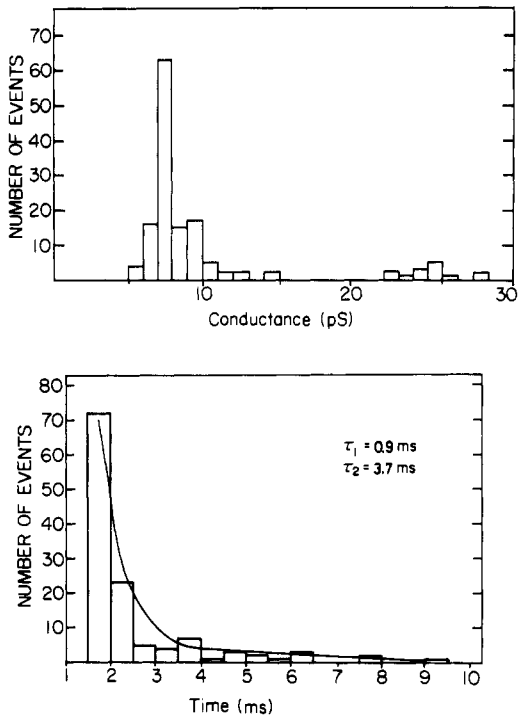

FIGURE 6: Conductance and open-time histograms constructed from antigen-induced single-channel events in the presence of identical solutions in the pipet and the well, both containing 0.5 M NaCl and 10 mM Tris-HCl, pH 7.4. Data were collected in three different experiments and are pooled together for the analysis.

Conductance measurements were also carried out under conditions where the reconstituted bilayers separated symmetrical, Ca^{2+}-free solutions containing 0.5 M NaCl and 10 mM Tris-HCl. These experiments were found to be relatively difficult to perform since, in the absence of calcium, the micropipet-supported bilayers are less stable and tend to break down during the experiment (Coronado, 1985). Our results, nevertheless, confirmed that, under these conditions as well, antigen induces channel activity. The channel events observed in these symmetrical sodium solutions, like those detected with calcium, appear isolated and scattered in time, with long intervals without activity. Figure 6 shows the conductance and open-time histograms derived from three different experiments performed under these conditions. The conductance histogram (Figure 6, upper panel) shows a main peak at 7–8 pS, as compared to the 4.5–5 pS observed in the presence of 100 mM Ca^{2+}. Significantly, also under these conditions, a second, well-defined peak appears at a higher conductance, in the range of 22–26 pS, accounting for <10% of the events. The open-time histogram (Figure 6, lower panel) shows that, as in the experiments with symmetrical 100 mM calcium, most of the events have open times in the range 1.5–5 ms. However, in contrast to the earlier case, events with open times longer than 6 ms are very scarce and none was detected with an open time longer than 10 ms. The data presented in this histogram were fitted to the sum of two exponentials with average open times of 0.9 ms (similar to the 1.2 ms in Figure 2) and 3.7 ms (i.e., markedly smaller than the 17.2 ms derived from Figure 2).

DISCUSSION

The results presented in this report show unequivocally that calcium ions are the main current-carrying ions through the channels opened upon aggregation of Fc_ϵ receptor–IgE complexes in bilayers containing the latter complex and the channel-forming protein. Two distinct types of conductance events are induced by aggregation under each of the four different experimental protocols employed in this study: (1) a small-conductance channel, which is by far the most frequent event, accounting for more than 90% of all the events observed in each individual experiment; (2) a channel with a relatively larger conductance, which, though accounting for no more than 5–10% of all events, is observed in practically each of the experiments performed.

The small-conductance channel is selective for calcium, irrespective of the presence or absence of monovalent cations. Under these conditions, the conductance of this channel shows only a limited dependence on calcium concentration: 4–5 pS in the presence of symmetrical solutions containing 100 mM $CaCl_2$ only; 3 pS in the presence of a $[Ca^{2+}]$ gradient of 4 orders of magnitude and symmetrical 150 mM NaCl or KCl concentration. We have earlier determined a value of 1–2 pS for the conductance of this channel [between *identical* solutions containing 1.8 mM $CaCl_2$ and 145 mM NaCl; Corcia et al. (1986)]. The relatively small differences in single-channel conductance values observed are most probably a reflection of the different experimental conditions employed.

The selectivity for calcium of the small-conductance channel is demonstrated by the experiments performed in the presence of a calcium gradient across the bilayer. In these experiments, sodium and chloride ions are present at the same concentration on both sides of the bilayer, so that their reversal potential is zero. The reversal potential for calcium can therefore be calculated from the Nernst equation:

$$V_{\text{reversal}} = \frac{RT}{zF} \ln \frac{[Ca^{2+}]_o}{[Ca^{2+}]_i} = 29.2 \log \frac{[Ca^{2+}]_o}{[Ca^{2+}]_i}$$

Introducing the values $[Ca^{2+}]_o$ = 1.8 mM and $[Ca^{2+}]_i$ = 0.1 μM employed in our experiments, the calculated value for the reversal potential is V_{reversal} = 124.3 mV. The experimental values obtained from the intercepts of the current–voltage (I–V) plots constructed for this low-conductance channel are $V_{(\text{reversal})}$ = 134.5 ± 11.5 mV in the presence of sodium and 125.5 ± 12.9 mV in the presence of potassium. These values agree very well with those calculated above by inserting the appropriate Ca^{2+} concentrations into the Nernst equation. Hence, we may conclude that the small-conductance channel is indeed calcium-specific. This conclusion could also be tentatively reached from the experiments carried out in the presence of $CaCl_2$ alone. However, the possibility that under the latter experimental conditions the channel would be permeable to chloride ions could not be excluded. Neither could be eliminated the possibility that calcium was passing through a channel selective for another cation (either sodium or potassium). The present results obtained in the presence of a calcium gradient, primarily the agreement between the calculated and the observed values of the reversal potential, clearly exclude these possibilities and establish the calcium specificity of the Fc_ϵ receptor operated channels.

The second type of antigen-induced channel events observed in this study has a higher conductance and was much less frequent than the one discussed above. On the average, 5–10% of the events observed in each experiment fall into this class, implying that only a few such events can be observed during an experimental period of 10–15 min. The conductance of this channel is 10–12 pS in symmetrical 100 mM $CaCl_2$ solutions. Higher values are observed in the presence of the calcium gradient: 21.7 pS with sodium as the monovalent cation and 15.6 pS with potassium. The scarcity of this type of events makes any conclusion on its characteristics or significance only tentative at this stage.

With certain reservations, the selectivity of this channel can also be derived from the reversal potential determined in ex-

periments done in the presence of the calcium gradient. The classical Goldman equation has been derived for monovalent ions only and cannot be employed for analysis of these data since the concentrations of calcium have to be taken into account. Starting from the Goldman–Hodgkin–Katz equation (Lee & Tsien, 1982; Bowman & Baglioni, 1984), it can be shown that for the case where both calcium and a monovalent cation are considered, if the monovalent cation concentration is identical on both sides of the membrane, the selectivity ratio is given by

$$\frac{P(Ca^{2+})}{P(M^{+})} = \frac{[M^{+}][1 - \exp(2FV_r/RT)]}{4[[Ca^{2+}]_i \exp(2FV_r/RT) - [Ca^{2+}]_o]}$$

where $P(X^{n+})$ is the permeability coefficient of a given cation, $[M^+]$ is the concentration of the monovalent cation (in the present case, either sodium or potassium), V_r is the reversal potential and F, R, and T have their conventional meaning. In deriving this expression one assumes that the difference between external and internal surface potentials is small. In our case, $[M^+]$ = 150 mM for the experiments with either NaCl or KCl. Using the value of V_r = 16 mV derived from Figure 6, one obtains $P(Ca^{2+})/P(M^+)$ = 53. Inclusion of a surface potential contribution in the equation would decrease this ratio. This permeability ratio is much smaller than the values obtained for the calcium channels in ventricular myocytes [permeability ratios >1000; Lee and Tsien (1982); McDonald et al. (1986)] and in bovine cardiac sarcolemma [ratio >2000, Rosenberg et al. (1986)], but is still higher than the value reported for the adenine nucleotide activated calcium channel present in sarcoplasmic reticulum [permeability ratio of 10; Smith et al. (1985)]. This selectivity value implies that, under the given experimental conditions, the second type of conductance events observed is moderately selective for calcium and does not discriminate appreciably between the monovalent cations present.

Regarding the conductance under an electrochemical gradient, Mohr and Fewtrell (1987) have recently shown that in potassium-depolarized RBL-2H3 cells antigen-induced calcium influx was abolished. Since they have observed a decrease in the basal level of cellular calcium under these conditions, their observations suggest that the maintained calcium concentration gradient across the plasma membrane was not sufficient to support any net influx, nor could it maintain the steady-state concentration. The present study suggests that the isolated channel is still operating under a calcium gradient at zero applied potential (Figure 5), so that the abolished influx is not due to a depolarization-dependent channel closure. The cause(s) for the influx inhibition by the cellular depolarization may be related to regulatory events that remain to be clarified.

In solutions where the only cation present is sodium, Fc_ϵR-gated channels also exhibit two conductance levels. The proportion of events with low and high conductances is similar to that observed in the presence of calcium. The experiments performed in sodium chloride solutions show that the small-conductance channel has, under these conditions, a conductance of 8 pS, while the high-conductance channel has a value of 25 pS. From this point of view, Fc_ϵR-gated channels exhibit properties similar to those observed for other calcium channels. Under different experimental conditions, calcium channels were shown to be highly selective and exclude monovalent cations (Lee & Tsien, 1982; Fukushima & Hagiwara, 1985; McCleskey & Almers, 1985). However, in the absence of extracellular calcium (or when this ion is present at micromolar concentrations) they allow passage of various monovalent cations. This behavior has been observed in voltage-gated calcium channels present in different tissues of both vertebrates and invertebrates. Comparison of the open-time characteristics of the Fc_ϵR-gated channels in the presence or absence of calcium shows a further distinction between the two modes of channel function. The slow exponential (representing the fraction of events that stays open for longer periods of time) has a longer average time in the presence of calcium than in its absence. This may suggest that calcium stabilizes the open-channel state more effectively than sodium ions, either directly or through effects on the lipid bilayer.

Antigen-induced $^{22}Na^+$ uptake has been shown to occur in RBL-2H3 cells suspended in calcium-free medium (Kanner & Metzger, 1984), leading to the suggestion that sodium employs the same pathway as calcium to cross the plasma membrane upon antigen stimulation. In bilayers formed from RBL-2H3 plasma membrane vesicles, antigen-induced channel activity in the absence of calcium has already been observed (Mazurek et al., 1984). These results, however, did not provide evidence that the sodium and calcium influx may proceed through one and the same channel, since the plasma membranes could, in principle, contain different types of channels. The present results show that, in the absence of external calcium, sodium can indeed enter the cells through Fc_ϵR-gated channels.

We have previously brought evidence (Corcia et al., 1986; Pecht et al., 1986) that only two protein entities incorporated into the reconstituted bilayers (the Fc_ϵ receptor complex and the channel-forming protein) are necessary and sufficient components for observing antigen-induced channels. Since bilayers reconstituted with the Fc_ϵ receptor complex alone did not show channel activity in response to cross-linking, we concluded that the receptor was not the channel-forming protein. In the present study, we have shown that this Fc_ϵR-gated channel is selective for calcium against monovalent cations and, as is the case with other types of calcium channels (Fukushima & Hagiwara, 1985; Hess & Tsien, 1984; Mazzanti & DeFelice, 1986), allows passage of sodium in the absence of calcium in the solution.

Recently, it has been reported (Lindau & Fernandez, 1986a,b) that, in rat peritoneal mast cells, antigen-induced degranulation may proceed without the involvement of calcium channels. Using the slow whole cell configuration of the patch clamp methodology, no changes could be detected in the cell membrane conductance, preceding antigen-induced degranulation, that may be ascribed to the opening of calcium channels. One possible explanation for this observation may reside in the low conductance changes expected to occur upon antigen stimulation. It is conceivable that the rather small calcium channel conductance we observe in reconstituted bilayers was masked in the single-cell measurements by the high background of other channels present in the cell membrane. The following approximate calculations illustrate this point: In the series of experiments performed in the presence of a Ca^{2+} concentration gradient (Figure 6), the average conductance of the Fc_ϵR-gated calcium channel was 3 pS. We usually observe 50–100 opening events in a 10-min period. Hence, assuming that there is on the average only one functional channel in every reconstituted bilayer, this channel may open on the average 8 times/min. Most of the observed events are very short-lived (average open time of 1 ms), while some (but not many) remain open for longer periods (e.g., 17 ms average open time in Figure 2). Assuming further a combined average open time of 3 ms, then any channel would stay open 24 ms/min (0.4 ms/s). If the channels open independently, one needs to have 2500 active channels present per cell in order

to have one channel open at any given time. From binding and isolation measurements, the abundance of channel-forming protein molecules in the RBL cells is in the range of 10^4 per cell (Hemmerich & Pecht, 1988). Thus, on the average, there would be four open channels ($10^4/2500$) at any time. These channels will then lead to an increase of only 12 pS (four channels of 3 pS) in the conductance of the whole cell membrane. Conductance increases of this order of magnitude were in fact observed in the above-mentioned study (Lindau & Fernandez, 1986a); however, this was rationalized in a different way. These expected changes of membrane conductance due to the opening of antigen-induced calcium channels are much smaller than the values observed in adrenal chromaffin cells (Neher & Marty, 1982). In these calls, conductance changes in the range of 800–2000 pS, due to the opening of voltage-activated calcium selective channels, have been observed prior to exocytosis.

The above calculations also lead to values of antigen-induced calcium influx that fall into the range of those actually observed in RBL-2H3 cells. The number of ions passing through the above-described calcium channels per second can now be calculated. The expression for this flux is

$$\text{flux} = N \cdot G \cdot V / z \cdot F$$

where G is the average increase in membrane conductance induced by antigen (12 pS), V is the cell membrane potential, N is Avogadro's number, z is the ionic valence, and F is Faraday's constant. Taking a value of −60 mV for the cell membrane potential, one predicts a calcium influx of 0.2×10^7 ion/s. Measurements of $^{45}Ca^{2+}$ influx in RBL cells yield initial rates of 0.85×10^7 [calculated from Mohr and Fewtrell (1987)], 0.5×10^7 (Crews et al., 1981), or 1.3×10^7 (Ran & Rivnay, 1988) Ca^{2+} ions per cell per second, a range of values quite compatible with our calculations.

A molecular description of the channel-forming species responsible for each of the two types of channel events observed in this study is at present rather limited. It can be suggested that the small-conductance channel is induced by aggregation of at least two $Fc_\epsilon R$ units. The minor population of channels with higher conductance might be related to the formation of larger aggregates or to some modification of the proteins that can take place during purification. The former possibility may be examined by using cross-linking agents that induce structurally better defined aggregates and will be the subject of a separate study.

Several models have been proposed to explain the exquisite selectivity for calcium of the channels observed in different cells (Kostyuk et al., 1983; Hess & Tsien, 1984; Iijima et al., 1986). However, the properties of the channel emerging from our present results do not fit the predictions of any of these models and indicate that this receptor-operated calcium channel is essentially different from other calcium channels reported so far. The small-conductance $Fc_\epsilon R$-gated channel described here exhibits very limited dependence on calcium concentration, and at least in the range of voltages applied in this study, its ion selectivity shows no voltage dependence. Another difference between the $Fc_\epsilon R$-activated calcium channel and other known calcium channels is the low frequency of channel openings observed in our experiments. This means that the channels dwell for long periods of time in the closed, nonconducting state, under our experimental conditions.

ACKNOWLEDGMENTS

We thank Hamutal Aloni and Sari Wacks for their technical help and Prof. I. Z. Steinberg for valuable comments. B.R. is the incumbent of the Alan Dixon Career Development Chair in Cancer Research, established by the Chicago Committee for the Weizmann Institute of Science.

Registry No. Ca, 7440-70-2; Na, 7440-23-5; K, 7440-09-7.

REFERENCES

Beaven, M. A., Moore, J. P., Smith, G. A., Hesketh, S. T. R., & Metcalfe, J. C. (1984) *J. Biol. Chem. 259*, 7138–7142.

Befus, D. A., Denburg, J. A., & Bienenstock, J., Eds. (1986) *Mast Cell Differentiation and Heterogeneity*, Raven, New York.

Bowman, C. L., & Baglioni, A. (1984) *J. Theor. Biol. 108*, 1–29.

Cochrane, D. E., Distel, D. L., Lansman, J. B., & Peterson, B. M. (1982) *J. Physiol. (London) 382*, 423–435.

Corcia, A., & Babila, T. (1985) *Biophys. J. 47*, 141a.

Corcia, A., Schweitzer-Stenner, R., Pecht, I., & Rivnay, B. (1986) *EMBO J. 5*, 849–854.

Coronado, R. (1985) *Biophys. J. 47*, 851–857.

Coronado, R., & Latorre, R. (1983) *Biophys. J. 43*, 231–236.

Crews, F. T., Morita, Y., McGivney, A., Hirata, F., Siraganian, R. P., & Axelrod, R. (1981) *Arch. Biochem. Biophys. 212*, 561–571.

Douglas, W. W., & Ueda, Y. (1973) *J. Physiol. (London) 234*, 97–98.

Eccleston, E., Leonard, B. J., Lowe, J. S., & Wellford, H. J. (1973) *Nature (London) 244*, 73–76.

Enis, M., Truneh, A., White, J. R., & Pearce, F. L. (1980) *Int. Arch. Allergy Appl. Immunol. 62*, 467–471.

Fabiato, A., & Fabiato, F. (1975) *J. Physiol. (Paris) 75*, 463–505.

Fernandez, J. M., Neher, E., & Gomperts, B. D. (1984) *Nature (London) 312*, 453–455.

Fewtrell, C., Kessler, A., & Metzger, H. (1979) *Adv. Inflammation Res. 1*, 205–221.

Foreman, J. C. (1981) *Annu. Rev. Pharmacol. Toxicol. 21*, 63–81.

Foreman, J. C., & Mongar, J. L. (1972) *J. Physiol. (London) 224*, 753–769.

Fukushima, Y., & Hagiwara, S. (1985) *J. Physiol. (London) 358*, 255–284.

Gomperts, B. D., & Fewtrell, C. (1986) in *Molecular Mechanisms of Transmembrane Signalling* (Cohen, P., & Houslay, M. D., Eds.) pp 377–409, Elsevier, Amsterdam.

Hemmerich, S., & Pecht, I. (1988) *Biochemistry* (preceding paper in this issue).

Hess, P., & Tsien, R. W. (1984) *Nature (London) 309*, 453–456.

Holowka, D., & Metzger, H. (1982) *Mol. Immunol. 19*, 219–227.

Iijima, T., Ciani, S., & Hagiwara, S. (1986) *Proc. Natl. Acad. Sci. U.S.A. 83*, 654–658.

Kagawa, Y., & Racker, E. (1971) *J. Biol. Chem. 246*, 5477–5487.

Kanner, B. I., & Metzger, H. (1984) *J. Biol. Chem. 259*, 10188–10193.

Kostyuk, P. G., Mironov, S. L., & Shuba, Y. M. (1983) *J. Membr. Biol. 76*, 83–93.

Lee, K. S., & Tsien, R. W. (1982) *Nature (London) 297*, 498–501.

Lichtenstein, L. M., & Osler, A. G. (1964) *J. Exp. Med. 120*, 507–530.

Lindau, M., & Fernandez, J. M. (1986a) *Nature (London) 319*, 150–152.

Lindau, M., & Fernandez, J. M. (1986b) *J. Gen. Physiol. 88*, 349–368.

Liu, F.-T., Bohn, J. W., Ferry, E. L., Yamamoto, H., Molinaro, C. A., Sherman, L. A., Klinman, N. R., & Katz, D. H. (1980) *J. Immunol. 124*, 2728-2736.
Mazurek, N., Schindler, H., Schurholz, T., & Pecht, I. (1984) *Proc. Natl. Acad. Sci. U.S.A. 81*, 6841-6845.
Mazzanti, M., & DeFelice, L. J. (1986) *Biophys. J. 49*, 173a.
McCleskey, E. W., & Almers, W. (1985) *Proc. Natl. Acad. Sci. U.S.A. 82*, 7149-7153.
McDonald, T. F., Cavalie, A., Trautwein, W., & Pelzer, D. (1986) *Pfluegers Arch. 406*, 437-448.
Metzger, H., Alcaraz, G., Hohman, R., Kinet, J.-P., Pribluda, V., & Quarto, R. (1986) *Annu. Rev. Immunol. 4*, 419-471.
Mohr, F. C., & Fewtrell, C. (1987) *J. Cell Biol. 104*, 783-792.
Mongar, J. L., & Schild, H. O. (1958) *J. Physiol. (London) 140*, 272-284.
Neher, E., & Marty, A. (1982) *Proc. Natl. Acad. Sci. U.S.A. 79*, 6712-6716.
Nelson, M. T. (1986) in *Ion Channel Reconstitution* (Miller, C., Ed.) pp 507-522, Plenum, New York.
Pecht, I., Dulič, V., Rivnay, B., & Corcia, A. (1986) in *Mast Cell Differentiation and Heterogeneity* (Befus, A. D., Denburg, J. A., & Bienenstock, J., Eds.) pp 301-312, Raven, New York.
Ran, S., & Rivnay, B. (1988) *Eur. J. Biochem. 171*, 693-701.
Reck, B., Sagi-Eisenberg, R., & Pecht, I. (1986) *J. Allergy Clin. Immunol.* (Proc. 12th ICACI) *78*, 164-170.
Rivnay, B., Rossi, G., Henkart, M., & Metzger, H. (1984) *J. Biol. Chem. 259*, 1212-1217.
Rosenberg, R. L., Hess, P., Reeves, J. P., Smilowitz, H., & Tsien, R. W. (1986) *Science (Washington, D.C.) 231*, 1564-1566.
Sagi-Eisenberg, R., Lieman, H., & Pecht, I. (1985) *Nature (London) 313*, 59-60.
Saito, H., Okajima, F., Molski, T. F. P., Sha'afi, R. I., Ui, M., & Ishizaka, T. (1987) *J. Immunol. 138*, 3927-3934.
Seldin, D. C., Adelman, S., Austen, K. F., Stevens, R. L., Hein, A., Caulfield, J. P., & Woodburg, R. G. (1985) *Proc. Natl. Acad. Sci. U.S.A. 82*, 3871-3875.
Smith, J. S., Coronado, R., & Meissner, G. (1985) *Nature (London) 316*, 446-449.

Kinetic Analysis of Covalent Hybrid Plasminogen Activators: Effect of CNBr-Degraded Fibrinogen on Kinetic Parameters of Glu_1-Plasminogen Activation†

Pauline P. Lee, Robert C. Wohl, Irena G. Boreisha, and Kenneth C. Robbins*
Joint Section of Hematology/Oncology, Department of Medicine, University of Chicago Medical Center/Michael Reese Hospital and Medical Center, Pritzker School of Medicine, The University of Chicago, Chicago, Illinois 60616
Received March 11, 1988; Revised Manuscript Received June 1, 1988

ABSTRACT: The kinetic parameters of three activator species of Glu_1-plasminogen (Glu_1-Plg) were compared in their reaction at pH 7.4 and 37 °C, in the presence and absence of CNBr-digested fibrinogen (CNBr-Fg). The urokinase- (u-PA-) derived covalent hybrid activator Pln_A-u-PA_B had an apparent Michaelis constant (K_{plg}) of 7.44 μM, a catalytic rate constant (k_{plg}) of 51.1 min^{-1}, and a second-order rate constant (k_{plg}/K_{plg}) of 6.87 μM^{-1} min^{-1}. The tissue plasminogen activator (t-PA) derived covalent hybrid activator Pln_A-t-PA_B was characterized by a K_{plg} of 3.33 μM, a k_{plg} of 1.03 min^{-1}, and a k_{plg}/K_{plg} of 0.309 μM^{-1} min^{-1}. The k_{plg}/K_{plg} values for the parent u-PA and t-PA activators were 6- and 16-fold higher than the respective hybrids, mainly due to an ~10-fold increase in the apparent K_{plg} for the hybrids. In the presence of CNBr-Fg, the increase of the k_{plg}/K_{plg} values for u-PA and its hybrid was 1.1-fold, but for t-PA and its hybrid, the increases were 7- and 12-fold, respectively. In both the absence and presence of CNBr-Fg, activator t-PA_B had an apparent K_{plg} of 19.1 and 27.6 μM and a k_{plg} of 2.9 and 5.0 min^{-1}, respectively. The increase in the k_{plg}/K_{plg} value with CNBr-Fg was 1.2-fold. The streptokinase- (SK-) derived activators Glu_1-plasmin·SK (Glu_1-Pln·SK), Val_{442}-Pln·SK, and Val_{561}-Pln·SK had apparent K_{plg} values of 0.458, 0.268, and 0.121 μM and k_{plg} values of 20.0, 126.0, and 63.3 min^{-1}, respectively. In the presence of CNBr-Fg, the first two activators showed an ~1.4-fold increase and the last showed a 1.4-fold decrease in their k_{plg}/K_{plg} values. The catalytic efficiency (k_{plg}/K_{plg}) of the various activator species fell in the decreasing order SK > u-PA > t-PA, in either the presence or absence of CNBr-Fg. CNBr-Fg enhanced significantly the activities of only two activators, t-PA and Pln_A-t-PA_B.

Plasmin (Pln)[1] is the principal plasma enzyme responsible for the dissolution of blood clots. It is formed from plasminogen (Plg) by an activation system that includes tissue plasminogen activator (t-PA), urokinase (u-PA), or the plasmin(ogen)·streptokinase (SK) species. Pln, Plg, and the activators all share the common characteristics of having a fibrin-binding domain and a catalytic domain (Bachmann,

† This work was supported in part by National Institutes of Health Grant HL-34276.
* Address correspondence to this author at the Joint Section of Hematology/Oncology, Michael Reese Hospital and Medical Center, Lake Shore Drive at 31st St., Chicago, IL 60616.

[1] Abbreviations: CNBr-Fg, CNBr-degraded fibrinogen; Plg, plasminogen; Pln, plasmin; Pln_A, NH_2-terminal plasmin-derived heavy A chain; SK, streptokinase; u-PA, urokinase; u-PA_B, COOH-terminal urokinase-derived catalytic B chain; t-PA, tissue plasminogen activator; t-PA_B, COOH-terminal tissue plasminogen activator derived catalytic B chain; HMW, high molecular weight; LMW, low molecular weight; P_i, inorganic phosphate; IU, international units established by World Health Organization for SK, t-PA, and u-PA; S-2251, H-D-valyl-L-leucyl-L-lysyl-*p*-nitroanilide.

0006-2960/88/0427-7506$01.50/0